The Meteoritical Society

Meteoritics & Planetary Science 50, Nr 3, 508–522 (2015)
doi: 10.1111/maps.12438

Observations of Martian layered ejecta craters and constraints on their formation mechanisms

Li LI[1,2], Zongyu YUE[1], Kaichang DI[1*], and Man PENG[1]

[1]State Key Laboratory of Remote Sensing Science, Institute of Remote Sensing and Digital Earth, Chinese Academy of Sciences, Beijing 100101, China
[2]University of Chinese Academy of Sciences, Beijing 100049, China
*Corresponding author. E-mail: dikc@radi.ac.cn

(Received 21 March 2014; revision accepted 23 January 2015)

Abstract–The formation mechanism of layered ejecta craters on Mars has remained a topic of intense debate since their discovery. In this study, we perform a global morphological analysis of Martian layered ejecta craters using Thermal Emission Imaging System (THEMIS) images and Mars Orbiter Laser Altimeter (MOLA) data. The study focuses on the ejecta morphologies and well-defined distal rampart characteristics associated with 9945 layered ejecta craters with a diameter greater than 1.5 km distributed across the entire Martian surface. Data analysis based on the new database provides new information on the distribution and morphological details of the three major layered ejecta morphologies (single layer ejecta [SLE], double layer ejecta [DLE], and multiple layer ejecta [MLE]). Global analysis is applied to the latitudinal distribution of characteristic parameters, including the ejecta mobility, lobateness values, and onset diameter. Our survey of the distribution and characteristics of layered ejecta craters reveals that strong correlations exist between ejecta mobility and latitude, and there is a latitudinal dependence of onset diameter. Our study of Martian layered ejecta craters provides more detailed information and insights of a connection between the layered ejecta morphologies and the subsurface volatiles.

INTRODUCTION

Impact craters are widely distributed on most terrestrial planets, and they play a major role in shaping planetary surfaces and elucidating the climatic and geologic history of planets. Martian impact craters exhibit a wide variety of ejecta morphologies, which differ significantly from their lunar and Mercurian counterparts. Impact craters on volatile-poor bodies like the Moon and Mercury typically show a blocky ejecta blanket with radial patterns and textures, and numerous secondary craters (Shoemaker 1962). Fresh Martian craters, however, are typically surrounded by layered ejecta deposits with relatively long runout distances that terminate in lobate distal ridges and ramparts (Carr et al. 1977). Based on the morphology of ejecta blankets, the Mars Crater Consortium recommended a standardized nomenclature for Martian ejecta morphologies, which can be generally divided into three main groups: layered (an ejecta blanket terminated by a distal rampart), radial (a radial pattern similar to that seen around lunar craters), and diverse (a combination of layered and radial patterns) (Barlow et al. 2000). In addition, pedestal craters are a subclass of Martian impact craters characterized by a crater perched near the center of a pedestal (mesa or plateau), surrounded by an often-circular, outward-facing scarp (Arvidson et al. 1976; Barlow et al. 2000; Kadish et al. 2009).

The most common ejecta morphologies on Mars are layered ejecta craters, which are typically surrounded by layered ejecta blankets with lobe-like ramparts and long runout flows. Martian layered ejecta craters have been classified into different types including single-layered ejecta (SLE) craters, double-layered ejecta (DLE) craters, and multiple-layered ejecta (MLE) craters (Barlow et al. 2000). SLE craters possess a single continuous ejecta layer surrounding the crater, and almost always terminate in a distal rampart. DLE craters have two ejecta layers, with one layer typically superimposed upon the other. DLE craters typically

display subdued ramparts in the outer facies which are morphologically distinct from those of SLE and MLE craters (Barlow 2005; Boyce and Mouginis-Mark 2006). MLE craters display two or more partial or complete ejecta layers surrounding the crater. Typically, only the outermost ejecta layer completely encircles the crater (Barlow 2005). This work focuses on the three major layered ejecta morphologies (Fig. 1).

The mode of emplacement of Martian layered morphologies has been a subject of intense study over the last few years. Three major formation models have been proposed to account for the layered ejecta morphologies (1) impact into near-surface volatile reservoirs (Carr et al. 1977; Mouginis-Mark 1979; Wohletz and Sheridan 1983; Stewart et al. 2001), (2) interaction of the ejecta curtain with the thin Martian atmosphere (Schultz and Gault 1979; Schultz 1992; Barnouin-Jha and Schultz 1998), (3) a combination of the two (Barlow 2005; Komatsu et al. 2007).

Observational data, laboratory experiments, and numerical modeling have provided important information about Martian layered ejecta structures. Martian layered ejecta morphologies were first recognized in Mariner 9 imagery (McCauley 1973). From the late 1970s through the late 1990s, the Viking image data were the main basis for the analysis of ejecta deposits around Martian craters (Mouginis-Mark 1979; Barlow and Bradley 1990). The morphologic features associated with the layered ejecta structures suggest that the layered ejecta deposits were fluidized at the time of their emplacement (e.g., Carr et al. 1977; Mouginis-Mark 1981; Barlow and Bradley 1990). Carr et al. (1977) proposed that layered ejecta deposits were emplaced as relatively thin ground hugging flows rather than simple ballistic ejecta. Evidence for this includes flow lines around obstacles, large runout distances, and the absence of ejecta on top and on the lee side of obstacles themselves (Carr et al. 1977). The observation that the diameter of the smallest crater displaying a layered ejecta morphology decreases as latitude increases (Kuzmin et al. 1988), the observed latitudinal variations of Martian ejecta morphologies (Mouginis-Mark 1979; Barlow and Bradley 1990), and the sinuosity variations among different ejecta types (Barlow 1994) all support the subsurface volatile hypothesis. Alternately, a number of laboratory experiments and numerical simulations show that thin Martian atmosphere serves as the medium in which the ejecta are entrained, and a vortex ring that develops from impact-induced turbulence in the atmosphere entrains, transports, and deposits fine-grained material from the ejecta curtain into a layered pattern (Schultz and Gault 1979; Schultz 1992; Barnouin-Jha and Schultz 1998; Barnouin-Jha et al. 1999a, 1999b). Barlow (2005) and Komatsu et al. (2007) raised the possibility that neither of these two models can exclusively explain all of the observations, and suggested that both subsurface volatiles and the atmosphere may contribute to the layered ejecta morphologies on Mars, but subsurface volatiles appear to be the major contributor.

In addition, Barnouin-Jha et al. (2005) investigated the similarities and differences between rampart crater emplacement and terrestrial and Martian landslides, and they proposed that fluidized ejecta result from dry granular flows that do not require any fluidizing agent. Baloga et al. (2005) presented a basic continuum flow model for the emplacement of distal rampart deposits on Mars, and suggested that only thin ejecta flows, moving at relatively low velocities, are needed to produce distal ramparts. Wada and Barnouin-Jha (2006) proposed that Martian fluidized ejecta deposits could be the result of simple granular flows. Boyce and Mouginis-Mark (2006) proposed that vortices from atmospheric interactions or base surges may have eroded inner layers and deposited material in the outer layers of DLE craters. Senft and Stewart (2008) used numerical simulations to explore and quantify the effects of icy surface and subsurface layers on Martian crater formation, they suggested that the presence of a weak ice layer caused variations in crater morphology, and Martian layered ejecta structures may be explained by the presence of icy layers. The existence of rampart craters on the Jovian satellite Ganymede indicates that an atmosphere is not required for ejecta fluidization and that the presence of volatiles in the subsurface is probably the dominant factor (Boyce et al. 2010). Osinski et al. (2011) suggested that the presence of multiple layers of ejecta is not unique to Mars but is a common outcome of the impact cratering process. They presented a unifying working hypothesis for the origin and emplacement of ejecta on the terrestrial planets, and they further proposed that the volatile content, cohesiveness of the uppermost target rocks, impact angle, and topography of the region surrounding the impact site will affect the final morphology and character of ejecta deposits. Weiss and Head (2013) proposed a glacial substrate model for the formation of DLE craters on Mars, which attributed many of the unusual characteristics of DLE craters to the presence of a glacial substrate (surface snow and ice layer) during the impact events. For these hypotheses, it is generally accepted that volatiles and/or atmosphere must have been involved in the emplacement of Martian layered morphologies. However, the exact role played by volatiles and the source of these volatiles for fluidization have been controversial for decades.

The geometry of layered ejecta deposits is important for understanding the mode of emplacement of layered

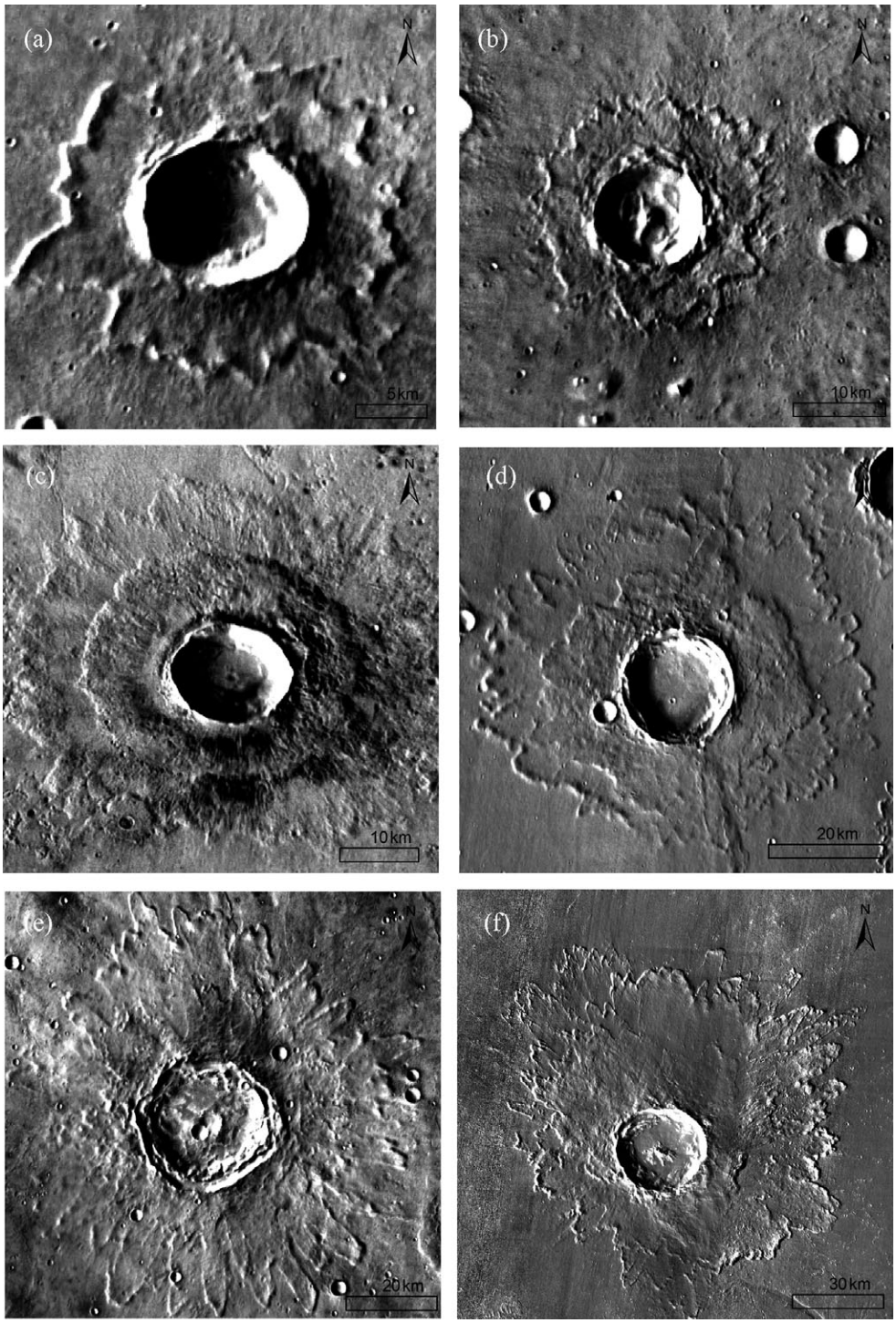

Fig. 1. Three types of Martian layered ejecta crater. Images are from THEMIS Daytime IR mosaics. a) SLE crater located at 29.0S, 141.2W; b) SLE crater located at 23.6N, 101.7E; c) DLE crater located at 34.7N, 120.5W; d) DLE crater located at 10.4N, 72.2W; e) MLE crater located at 14.8N, 66.1E; f) MLE crater located at 23.2N, 152.2W.

ejecta. Analyses of the global distribution and detailed morphology of layered ejecta craters are valuable for investigating the ejecta emplacement processes, as well as searching for spatial and/or temporal variations in ejecta characteristics that may be caused by latitude, altitude, or the properties of the target material. Catalogs of Martian craters have been developed for decades and there are three main completed crater

catalogs associated with ejecta blanket morphology. The first global database of Martian craters (Catalog 1.0) was created from Viking images in the late 1980s (Barlow 1988), in which 42,284 impact craters ≥5 km in diameter were cataloged; this is the basis for most other crater databases. As higher resolution images became available, Catalog 1.0 was revised using Mars Global Surveyor, Mars Orbiter Camera, and Mars Orbiter Laser Altimeter (MOLA) data and Odyssey THEMIS data (Barlow 2006). Robbins and Hynek (2012a, 2012b) created an independent Martian crater catalog with 384,343 craters ≥1 km in diameter across the entire Mars based on THEMIS Daytime IR data; the catalog contains detailed topographic information, interior morphology, and ejecta morphology for each crater. Barlow et al. (2014) used THEMIS visible (VIS) and daytime infrared (IR) images to conduct a global survey of the distribution and characteristics of low-aspect-ratio layered ejecta (LARLE) craters, which are characterized by a crater and normal layered ejecta pattern superposed on an extensive outer layer that terminates in a flame-like sinuous edges and deposits with anomalously high EM values. Their survey identified 140 LARLE craters ≥1 km in diameter in the ±75° latitude zone, and their database includes the central coordinates of the crater, the crater diameter, and the perimeter and area of the LARLE deposit. With regard to regional studies, Boyce et al. (2005) published a database containing 2269 craters of the Martian north plains including center location, crater diameter, and various height and depth measurements using MOLA topographic data. Our detailed investigation of previous databases and newly available images shows that a significant portion of these databases need to and can be updated with new data and more specific classification criteria.

This study endeavors to update the catalog of Martian layered ejecta craters, specifically identifying features that are most likely to have been formed as the result of subsurface volatiles. Using the updated catalog, we perform a global analysis of the morphologies of SLE, DLE, and MLE craters, including their locations, dimensions, ejecta mobility (EM), lobateness, etc. The details of crater morphology and correlations among morphology and latitude, diameter, and terrain can provide valuable information for understanding the formation mechanism of the ejecta blankets of layered ejecta craters.

METHODOLOGY

Our analysis focuses on Martian layered ejecta craters. We make no attempt to develop a theoretical model of emplacement of layered ejecta, but instead focus on the characteristic parameters, latitudinal distribution, and regional variations of the three major layered ejecta morphologies (Fig. 1).

We used THEMIS IR images (100 m pixel^{-1}) and MOLA data (463 m pixel^{-1}) for a global study of Martian layered ejecta craters. The coverage of the data set is adequate to include a large number of craters in our database and provide statistically valid results on a global scale. We integrated these data in ArcGIS software to manually locate all visible layered ejecta craters. After crater identification and classification, we extracted the characteristic parameters for each layered ejecta crater. The basic characteristic parameters of the layered ejecta craters involved crater type (SLE/DLE/MLE), latitude, longitude, diameter, depth, lobe number, ejecta perimeter, ejecta area, radial extent, etc; these measurements also allow the calculation of EM, lobateness (Γ), onset diameter (Dr), and depth/diameter ratio (d/D).

The maximum distance of the ejecta blanket from the crater rim is called the ejecta extent or runout distance and is used to describe quantitatively the EM by scaling with the radius of the crater (Mouginis-Mark 1979; Costard 1989; Barlow 2004).

$$\mathrm{EM} = \frac{\text{maximum ejecta extent from crater rim}}{\text{crater radius}} \quad (1)$$

Understanding the nature of the EM and the relationship between latitude and EM values may provide insights into impact conditions and the emplacement of layered ejecta.

Lobateness (Γ) is a measure of the sinuosity of the ejecta (Kargel 1989; Barlow 1994) and is defined using the ejecta perimeter and ejecta area as:

$$\Gamma = \frac{\text{ejecta parameter}}{2\sqrt{\pi \cdot \text{ejecta area}}} \quad (2)$$

A circular ejecta blanket will have a Γ value of 1.0, and higher Γ values correspond to more sinuous ejecta edges. The values of Γ are thought to be controlled by the rheological properties of the ejecta, and they can provide information about the physical nature of the ejecta and the flow process (Carr et al. 1977; Schultz 1992; Barnouin-Jha and Schultz 1998; Barlow 2006).

In a given area, a certain minimum diameter exists for craters which show fluidized ejecta blankets (Boyce and Witbeck 1980; Kuzmin 1980; Barlow and Perez 2003), called the onset diameter. Onset diameters can be used to estimate the excavation depth, which provides constraints on the depth of the subsurface volatile reservoirs (Boyce 1979; Kuzmin et al. 1988; Barlow et al. 2001).

The measurements of various morphometric parameters of the layered ejecta craters were conducted as follows. Positional data (latitude, longitude) are self-explanatory, and we used the basic parameter of Robbins and Hynek's database as a guide. Basic crater types follow the classification of Barlow et al. (2000), and include only SLE, DLE, and MLE craters. Extraction of ejecta blankets was achieved with the editing tools of ArcGIS by drawing a polyline tracing the visible rim of each layered ejecta blanket. For each crater, ejecta perimeter and ejecta area (exclude the area of the crater itself) were first computed, then lobateness can be calculated using Equation 2. When measuring EM of these craters, we fit a circle at approximately the median value between the maximum and minimum ejecta diameter ranges (e.g., Weiss and Head 2014), then the EM value can be calculated by the ejecta radius (exclude the crater radius itself) and the crater radius using Equation 1.

It is important to note that image resolution affects the smallest craters that can be reliably detected and measured. To ensure accurate classification, we only analyzed craters larger than 1.5 km in diameter, and focused on fresh layered ejecta craters (SLE, DLE, and MLE). The degraded pancake craters and pedestal craters were not included in this study because of the large uncertainties in their identification. After extracting the basic parameters and the derived parameters for each layered ejecta crater, we defined ranges of diameter and 10° latitude bins to infer population-width relationships from morphometric and latitudinal measurements.

OBSERVATION AND RESULTS

For this global analysis of craters ≥1.5 km in diameter that display layered ejecta morphologies, our database contains 9945 entries for SLE, DLE, and MLE craters; 4994 in the northern hemisphere and 4951 in the southern hemisphere (Fig. 2). The results for various morphometric parameters, the size distribution, and the latitudinal distribution of the layered ejecta craters are described in detail below.

SLE Craters

SLE craters display a single blanket surrounding the crater, and are the most common type of ejecta morphology on Mars. They have approximately symmetric ejecta blankets (Fig. 1). Of the 9945 craters with an ejecta morphology in this study, 7781 (78.2%) have SLE morphology. SLE craters dominate the ejecta morphologies across the entire planet.

In general, SLE craters are found at a variety of elevations (Fig. 3). The number of SLE craters in the northern hemisphere (3678) is slightly smaller than that of the southern hemisphere (4103). SLE craters have a globally oriented distribution that tends to increase in frequency toward the equator. Additionally, there may be minor concentrations of SLE craters in the regions of Tharsis Montes and Olympus Mons (Fig. 3).

The SLE morphology is associated with craters with diameters ranging from about 2 km to 66 km. They show a strong correlation with crater diameter and dominate the ejecta craters at diameters ≤20 km. The peak in frequency of SLE craters is at 6 km in diameter (Fig. 4).

From this analysis, we find that the EM values for SLE craters range between 0.12 and 6.31 with an average value of 1.26. There is a slight trend to higher EM values with increasing latitude. The mean EM is 1.2 near the equator and rises to 1.6–1.7 in the 50° to 70° latitude range in both northern and southern hemispheres (Fig. 5). Statistics are poor in the 80° to 90° latitude range because the number of identifiable layered ejecta craters is relatively small (Fig. 4). The Γ values of SLE craters vary from 1.01 to 3.10, with a mean value of 1.47, and no statistically significant variations in Γ with latitude are present. These results are consistent with those of Barlow (2006), whose research focused on impact craters in the northern hemisphere of Mars.

DLE Craters

DLE craters are a particularly enigmatic type of layered ejecta crater. They have a number of unique characteristics, including distinct striations on the inner and outer ejecta layers, unusual annular depressions at the base of the rim structural uplift, enhanced annular topography at the distal edge of the inner lobe, and a lack of secondary craters beyond the layered ejecta blanket (Fig. 1) (Barlow et al. 2000; Boyce and Mouginis-Mark 2006; Weiss and Head 2013).

DLE craters are observed at a variety of elevations and on a variety of terrain types. They account for 1167 of the 9945 craters with ejecta morphologies (11.7%). In the northern hemisphere, DLE craters (806, 69.1%) are generally present in the latitudinal bands from 30°N to 70°N, especially in the Acidalia, Arcadia, and Utopia Planitia regions. In the southern hemisphere, DLE craters (361, 30.9%) are relatively less concentrated than those in the northern hemisphere, and they are mainly present from 20°S to 60°S, especially in the regions of Thaumasis Highland, Terra Sirenum, and Hesperia Planum (Fig. 6). Our analyses are generally consistent with previous observations that DLE craters are concentrated in the topographically low regions between 35°N and 60°N (Barlow and Perez 2003) and they are

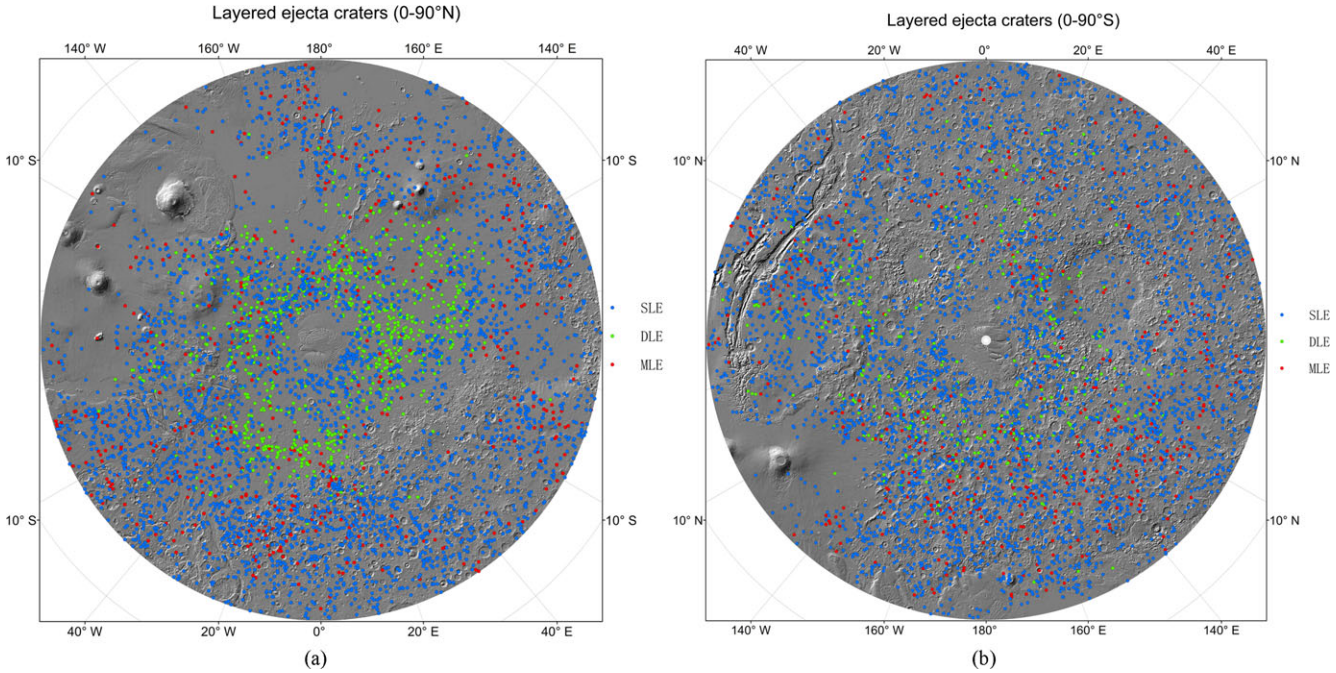

Fig. 2. Distribution of layered ejecta craters measured in this analysis. SLE (blue), DLE (green), and MLE (red) craters. a) The northern hemisphere; b) the southern hemisphere.

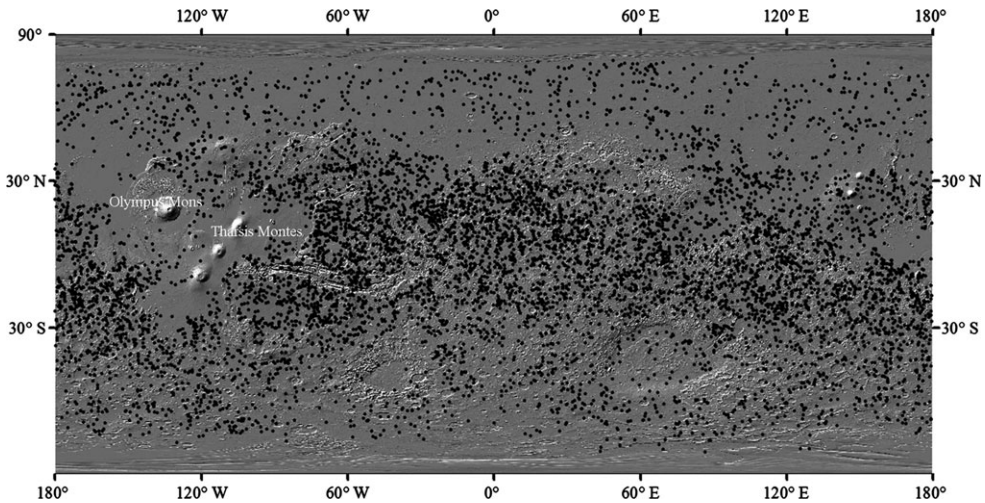

Fig. 3. Global distribution of SLE craters, with each point representing one SLE crater. The background is MOLA shaded relief map.

primarily located in the mid–high latitudes of Mars (Boyce and Mouginis-Mark 2006). Additionally, our results show that DLE are present in a larger range of latitudes (Fig. 6), and they are often in close proximity to other types of craters (i.e., SLE and MLE craters), especially in the southern hemisphere (Fig. 2).

The diameter range of DLE craters is similar to that of SLE craters, typically between 3 km and 50 km. The EM values for DLE craters vary from 0.29 to 4.15 for the inner ejecta layer, with an average value of 1.45. The outer layer is much more fluid, as shown by EM values ranging between 1.07 and 6.30 and an average value of 2.69. Figure 7 shows the latitudinal dependence of the EM and Γ values of DLE craters. It is obvious that the EM values are slightly higher in higher latitudinal zones for both the inner and outer layers of DLE craters (Fig. 7a).

The Γ values also vary between the inner and outer layers of DLE craters. The inner layer is relatively circular, with Γ values ranging from 1.04 to 2.55 and a

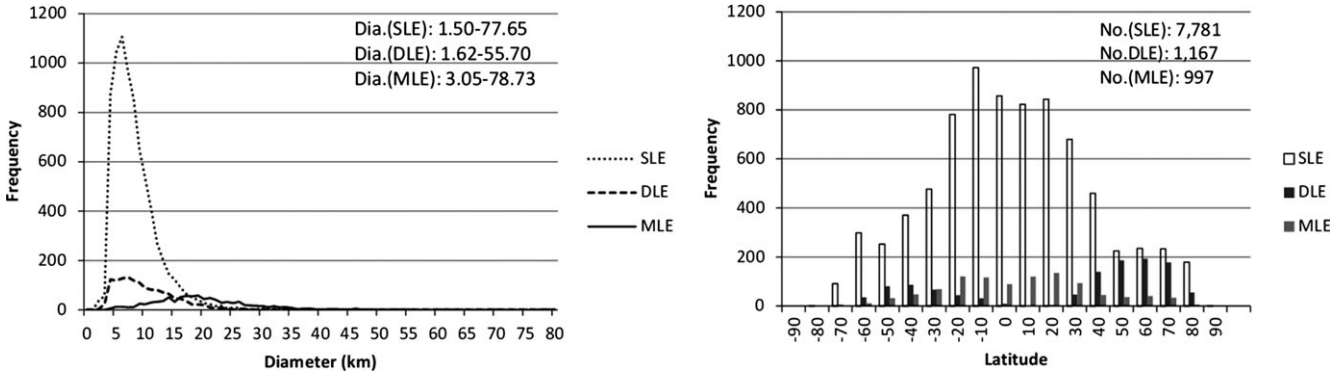

Fig. 4. Diameter frequency and latitude frequency for SLE, DLE, and MLE craters.

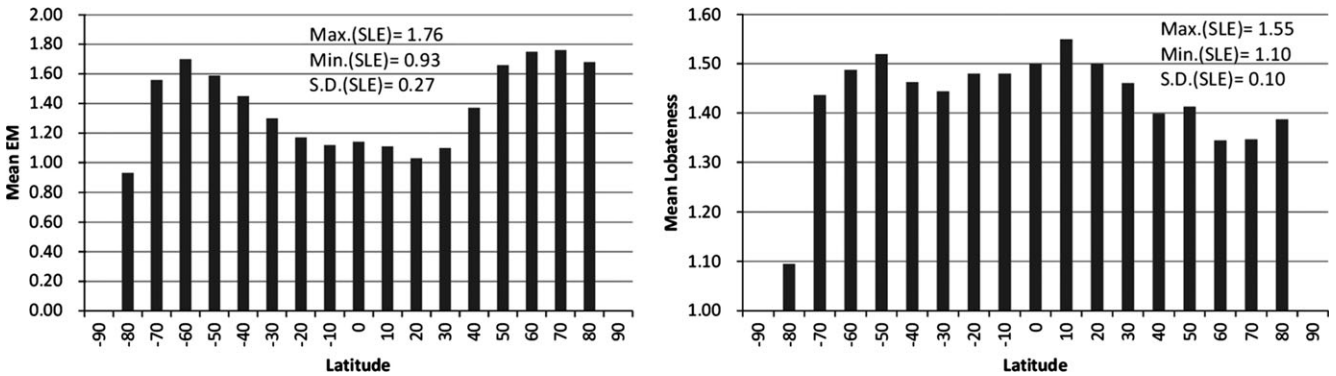

Fig. 5. The mean values of EM and Γ for SLE craters in 10° latitude bins.

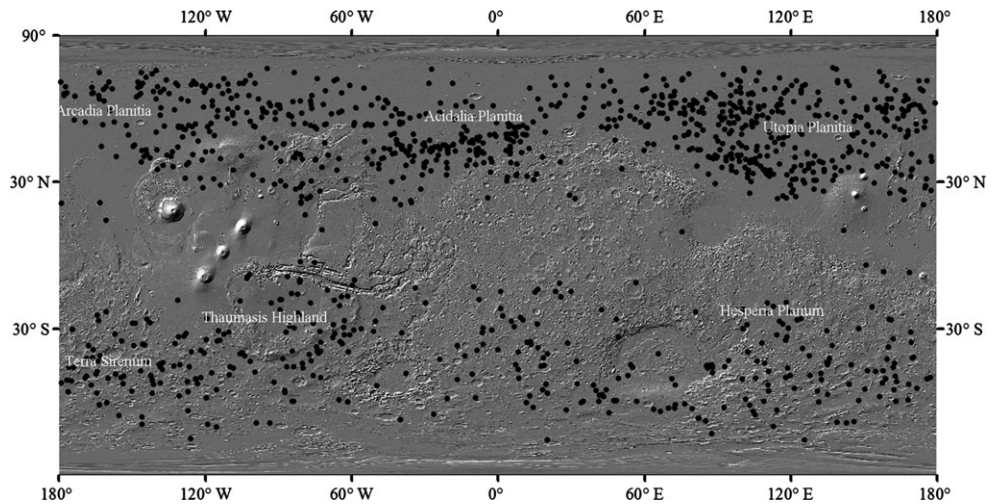

Fig. 6. Global distribution of DLE craters. Each point represents one DLE crater.

mean value of 1.45. The outer layer is slightly more sinuous, with values ranging from 1.06 to 3.71 and a mean value of 1.76. No large latitudinal variations in Γ values are observed, although the Γ values of the southern hemisphere are slightly larger than those of the northern hemisphere (Fig. 7). Our statistical values of Γ are larger than the findings of Barlow (2006), who obtained mean values of 1.09 and 1.14 for the inner and outer layer. This is probably due to the different research areas and databases used. Barlow's results focused on the northern hemisphere; this study shows that the Γ values of DLE craters in the southern

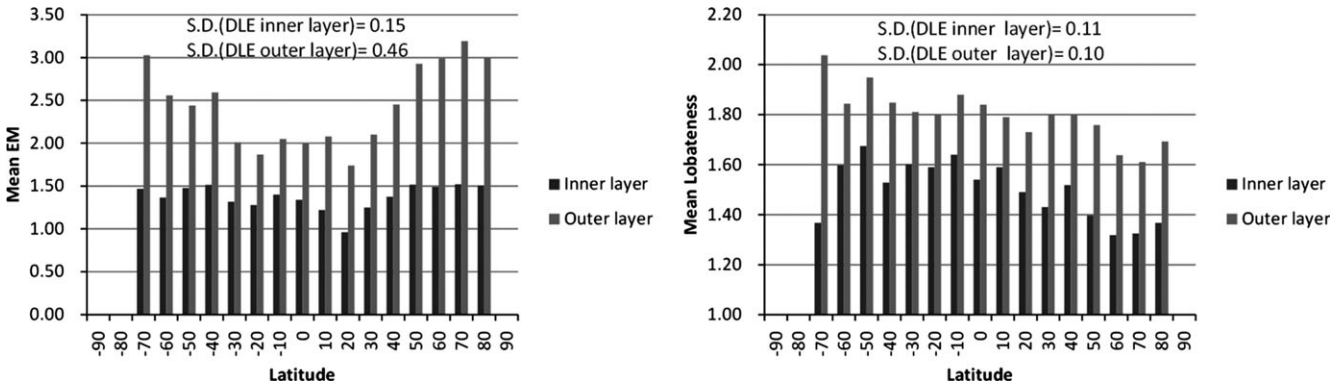

Fig. 7. The mean values of EM and Γ for the inner and outer layers of DLE craters in 10° latitude bins.

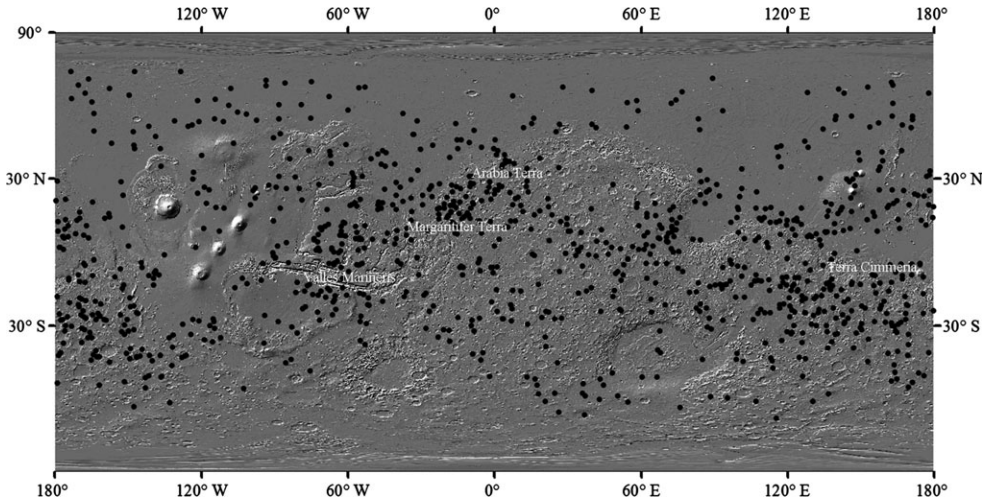

Fig. 8. Global distribution of MLE craters. Each point represents one MLE crater.

hemisphere are slightly larger than those of the northern hemisphere. In addition, higher resolution images enhance the precision of the ejecta perimeter and result in larger Γ values. These larger EM and Γ values for the outer layer in the two databases suggest that the outer layer ejecta material may have been much more fluid at the time of emplacement than that forming the inner layer.

MLE Craters

MLE craters have three or more ejecta layers, which can extend completely around the crater or be present only as partial segments (Fig. 1). They account for 997 of the 9945 craters in this study (10.1%). MLE crater diameters range from 2.5 km to 91 km, with typical values falling between 10 km and 45 km. The peak in frequency is at 16 km diameter (Fig. 4), and it appears to be difficult for a smaller crater to display MLE morphology.

MLE craters are concentrated in low and middle latitudes, and in particular along the dichotomy between the northern plain and the southern highland, especially in Arabia Terra, Terra Cimmeria, Margaritifer Terra, and the Valles Marineris region (Fig. 8), where valley networks and outflow channels are prevalent. This result generally agrees with the previous findings of Barlow and Perez (2003).

MLE craters display two or more partial or complete ejecta layers. Typically, only the outermost ejecta layer completely encircles the crater. Therefore, we compute EM and Γ values only for the outermost layer. In the northern hemisphere, the mean EM values of the outermost layer increase from 2.0 within the 0° to 30°N latitude zone to >2.5 at latitudes >40°N, and the results are similar for the southern hemisphere (Fig. 9). The mean values of EM and Γ for the outmost layeres of SLE, DLE, and MLE craters are shown in Fig. 10. In general, the EM values of SLE, DLE, and MLE craters are all smaller in the

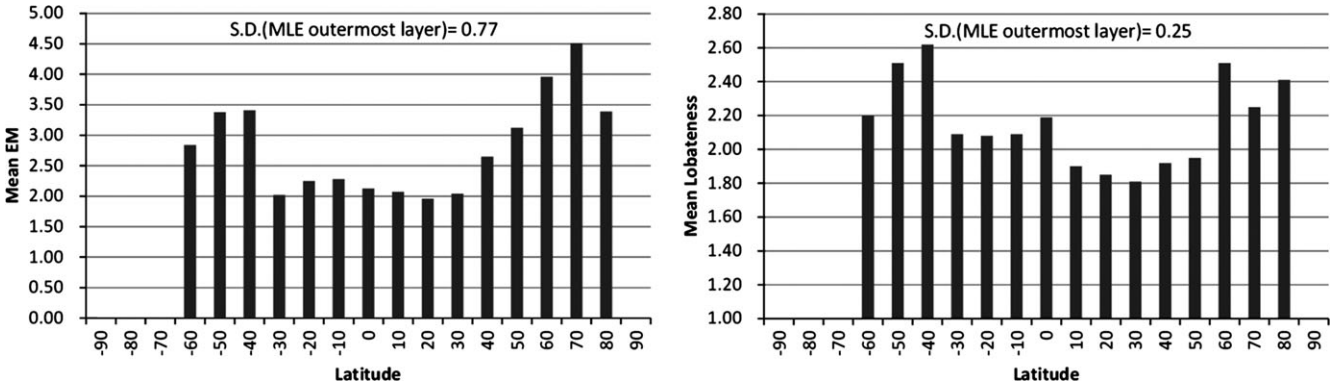

Fig. 9. The mean values of EM and Γ for the outermost layer of MLE craters in 10° latitude bins.

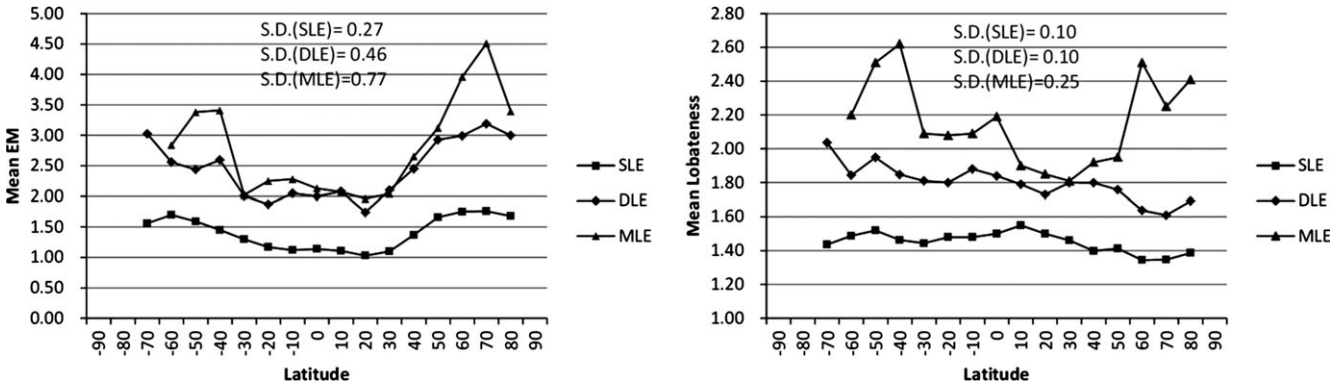

Fig. 10. Mean values of EM and Γ for the outermost layers of SLE, DLE, and MLE craters in 10° latitude bins.

equatorial region and larger at higher latitudes (Fig. 10).

The onset diameter and mean diameter for SLE, DLE, and MLE craters are shown in Fig. 11. The entire planet was subdivided into 10°×10° latitude-longitude squares and the smallest layered ejecta craters in each square were noted, then the average onset diameters in each latitude band were computed as onset diameter. It is obvious that the onset diameters for SLE, DLE, and MLE craters are all larger in the equatorial region (±30°) and smaller at higher latitudes (Fig. 11). Compared to the onset diameter, the mean diameter used in the study is the average value of crater diameter in each latitude band. The correlation between the mean diameter and crater type is notable, while there is no strong correlation between the mean diameter and latitude (Fig. 11).

DISCUSSION

Analyses of the global distribution and characteristics of layered ejecta craters are valuable for investigating the ejecta emplacement process, as well as obtaining insights into the spatial extents of the Martian surface and near-surface properties. Layered ejecta morphologies associated with fresh Martian impact craters have been attributed to both subsurface volatiles and the Martian thin atmosphere. In the following sections, we examine the results of our crater statistical analysis in the context of the layered ejecta formation mechanisms.

Crater Statistical Analysis

We conducted a comprehensive analysis of the global populations of layered ejecta craters and found 9945 layered ejecta craters with a diameter greater than 1.5 km distributed across the entire Martian surface. Our analysis shows that SLE, DLE, and MLE craters make up 78.2%, 11.7%, and 10.1%, respectively, of the layered ejecta craters on the Martian surface. The catalog of Martian layered ejecta craters produced by Barlow (2005) shows that approximately one-third of all Martian craters ≥5 km in diameter possess discernible ejecta blankets, with over 90% possessing layered ejecta that show single (SLE, 86%), double (DLE, 9%), or multiple (MLE, 5%) layer morphologies. Both catalogs confirm that the SLE crater is the dominant type of

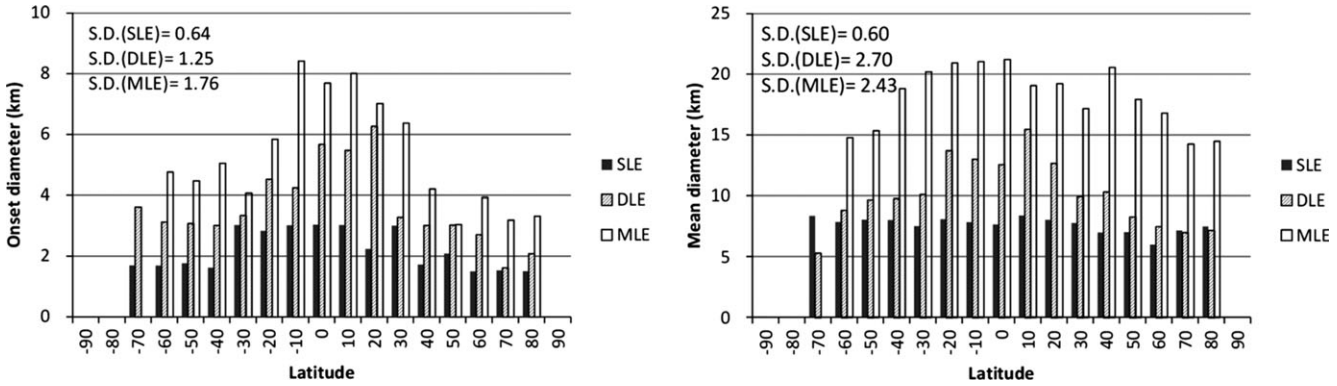

Fig. 11. The onset diameter and mean diameter for SLE, DLE, and MLE craters in 10° latitude bins.

layered ejecta morphology on Mars. However, our database contains smaller percentage of SLE craters and greater percentage of DLE and MLE craters, using high-resolution images and topographic data collected by the Mars Odyssey and Mars Global Surveyor.

Statistical analysis of the distribution of the three types of layered ejecta craters shows that there is no strong correlation between crater type and altitude (Mouginis-Mark 1979). For correlation between crater type and latitude, our results show that both SLE and MLE craters have broad latitudinal distributions, and they have a globally oriented distribution that tends to increase in frequency toward the equator. DLE craters are concentrated primarily in the mid–high latitudes of Mars, especially in topographic lows in the northern hemisphere. DLE craters are present in a larger range of latitudes (30°N to 70°N and 20°S to 60°S) than indicated by previous research results (Mouginis-Mark 1979; Barlow 2006).

Volatiles from either the atmosphere or vaporized subsurface ice are expected to increase EM, and thus regional variations in EM can provide information on the volatiles in those regions (Barlow 2006). Our analysis indicates that the EM values of layered ejecta craters are influenced by both crater type and latitude. In general, the EM values of SLE, DLE, and MLE craters are all smaller in the equatorial region and larger at higher latitudes (Fig. 10). This is in reasonable agreement with the findings of Barlow (2006), and may imply that the surface to the ice- or water-rich subsurface layers is deeper in the equatorial region than at higher latitudes (Clifford and Hillel 1983; Fanale et al. 1986; Mellon et al. 1997; Schorghofer and Aharonson 2005).

The morphometric parameters of SLE, DLE, and MLE craters are shown in Table 1. The mean EM value of 1.26 for SLE craters across the entire Martian surface is slightly smaller than the mean EM value of 1.45 for the DLE inner layer. However, the EM value of 2.69 for the DLE outer layer is much larger, implying that emplacement of DLE crater ejecta occurred in two different stages. The EM and Γ values of the outermost layer of the MLE craters are analogous to those of the single layer of SLE craters and the outer layer of DLE craters (Fig. 10). The MLE outermost layer has relatively high EM and Γ values, which may indicate that the ejecta material was very fluid at the time of emplacement.

One argument for the subsurface volatile origin of layered ejecta blankets is the observation that the onset diameter of layered ejecta craters decreases as latitude increases (Kuzmin et al. 1988). The onset diameter, along with the relationship between transient crater diameter and excavation depth can be used to estimate the depth to the volatile-rich layer. Average onset diameters of layered ejecta morphologies in the Martian equatorial region are typically between 4 and 7 km (Kuzmin et al. 1988). Studies based on high-resolution Viking imagery revealed that regional variations in onset diameter occur throughout the ±30° latitude zone; localized regions in Solis and Thaumasia Plana with smaller onset diameters of 3 km have been observed (Barlow et al. 2001). Higher resolution imagery from high resolution stereo camera revealed even smaller onset diameters in certain equatorial regions (Reiss et al. 2005). Our analysis of onset diameter is consistent with previous studies that there is a latitudinal dependence (Kuzmin et al. 1988; Barlow et al. 2001) and regional variations (Barlow et al. 2001; Barlow and Perez 2003) of the onset diameters.

The Effects of Subsurface Volatiles

It has been suggested that Martian fluidized ejecta craters hold historical information on subsurface water on Mars (Barlow 2005; Mouginis-Mark and Baloga 2006; Komatsu et al. 2007), because they probably resulted from volatiles in the target materials (Carr

Table 1. Statistics of the morphometric parameters of layered ejecta craters.

Ejecta morphology	EM_min	EM_max	EM_mean	Γ_min	Γ_max	Γ_mean
SLE	0.12	6.31	1.26	1.01	3.10	1.47
DLE (inner layer)	0.29	4.15	1.45	1.04	2.55	1.45
DLE (outer layer)	1.07	6.30	2.69	1.06	3.71	1.76
MLE (outermost layer)	1.17	10.57	2.53	1.20	4.66	2.03

et al. 1977; Mouginis-Mark 1979; Wohletz and Sheridan 1983; Stewart and Ahrens 2003), although atmosphere effects have also been proposed as an alternative explanation for these craters (Schultz and Gault 1979; Barnouin-Jha and Schultz 1998).

This study provides a generally consistent picture of Martian layered ejecta craters that can be summarized as follows. (1) There are several distinct layered ejecta morphologies on Mars; the most common types are SLE, DLE, and MLE craters. The average size and the size range are different for each type of layered ejecta craters; however, there is overlap in the size ranges of the three morphological types. (2) There is a latitudinal control on the occurrences of SLE, DLE, and MLE craters. SLE and MLE craters have a globally oriented distribution that tends to increase in frequency toward the equator, while DLE craters are primarily located in the mid–high latitudes of Mars. (3) For all the three types of layered ejecta craters, strong correlations exist between EM values and latitude, and higher EM values are correlated with higher longitude. (4) The Γ values vary little with latitude but increase with crater diameter. (5) There is a latitudinal dependence of the onset diameters for the three types of layered ejecta craters. These results can provide some insight into conditions that produce layered ejecta.

Previous studies have treated the ejecta facies of layered ejecta craters as ground-hugging continuum flows, similar to debris flows (Baloga et al. 2005; Barnouin-Jha et al. 2005), or granular flows (Wada and Barnouin-Jha 2006), or as a basal gliding unit (Barnouin-Jha et al. 2005; Weiss and Head 2014). In laboratory-scale experiments, Gault and Greeley (1978) attributed the EM values to the viscosity of the ejecta, and hence to the target material. This implies that if the crater ejecta were fluidized by subsurface volatiles, the EM value might provide an indicator of the relative target volatile content at the time of crater formation. If this were the case, our results, that layered ejecta craters in the mid-high latitudes of Mars have larger EM values than those in the equatorial region, may imply that the volatile content within the regolith target materials is higher in the mid-high latitudes. The atmospheric model for SLE formation argues that variations in atmospheric pressure and the distribution of fine-grained material will produce differences in the SLE morphology (Schultz and Gault 1979). Correlation between ejecta morphology and the physical state of subsurface led Barlow and Bradley (1990) to propose that the SLE crater results from impact into ice-rich material. The other model for SLE formation invokes impact into and vaporization of subsurface volatiles (Barlow 2006). Numerical modeling suggests that the model of impact into and vaporization of subsurface volatiles can reproduce many of the observed attributes of the SLE craters (Stewart et al. 2001; Senft and Stewart 2008). All observations are consistent with impact into subsurface volatile target materials being the dominant formation process of SLE craters. The maximum diameter of SLE craters may provide information about cryosphere thickness (Barlow and Perez 2003; Weiss and Head 2014). Clifford et al. (2010) argued that the two most important factors affecting the persistence of groundwater on Mars are the depth and pore volume of the cryosphere; they suggested that the zonally averaged thickness of the cryosphere may vary from 0–9 km at the equator to 10–22 km at the poles. Weiss and Head (2014) revealed the upper end of SLE crater diameter increases as a function of increasing latitude; they suggested that SLE craters form exclusively in an ice-saturated cryosphere which thickens toward the poles.

In this study, many of the regions where DLE craters are concentrated, particularly Utopia and Arcadia, are among the regions with the highest concentrations of H_2O based on the GRS results (Barlow and Perez 2003), indicating that target volatiles play an important role in the formation of DLE craters. The depositional chronology of the two layers of DLE craters is still controversial. Some authors have supposed that the inner layer overlies the outer layer, indicating successive deposition (Carr et al. 1977; Barlow and Perez 2003; Osinski 2006; Osinski et al. 2011; Harrison et al. 2013; Weiss and Head 2013; Wulf and Kenkmann 2014), while others have assumed that the inner layer was deposited first, followed by the outer layer (Mouginis-Mark 1981; Schultz 1992; Boyce and Mouginis-Mark 2006). The unique characteristics of DLE craters suggest that they were created through emplacement mechanisms that may be somewhat different from those of SLE and MLE crater ejecta. Costard and Kargel (1995) and Barlow and Perez (2003) have suggested that DLE craters may be formed in

areas where the subsurface has a high water content. Boyce and Mouginis-Mark (2006) suggested that DLE inner layer formed in the same way as SLE ejecta, perhaps involving both ballistic and flow processes, while DLE outer layer may have formed through a high-velocity outflow of ejecta caused either by vortex winds generated by the advancing ejecta curtain or by a base surge. Modeling by Senft and Stewart (2008) showed that impacting into a subsurface ice layer could explain the ejecta morphology of DLE craters. Weiss and Head (2013) explored a new hypothesis that numerous characteristics of Martian DLE craters can be plausibly explained by the presence of a glacial substrate (snow and ice layer) present during the impact events (Weiss and Head 2013). The larger EM and Γ values of DLE outer ejecta suggest that they were emplaced in two distinct stages and through two different processes. Barlow (2006) argued that the large EM values for DLE outer layer are difficult to obtain by vaporization of target volatiles alone and atmosphere may help to mobilize the flow to these large values. Her observations are consistent with the results from the study of DLE craters on Ganymede (an icy body with no significant atmosphere), where DLE outer layer have such low EM 1.3 (Neal and Barlow 2004) and 1.86 (Boyce et al. 2010), much smaller than those seen on Mars. Weiss and Head (2014) proposed that the anomalously large EM values of DLE craters forming in a surface ice layer could result from ejecta flight and deposition followed by sliding on a lubricating icy substrate. They found that the modeled sliding friction of DLE craters is an order of magnitude less than that of SLE and MLE craters. Jones and Osinski (2015) presented a regional model of subsurface layering on Mars derived from the observed diameter and EM trends of SLE and DLE craters, and they suggested that DLE craters form through impact into a layered target of varying viscosities. The attributes of DLEs in equatorwards of 30° are potentially consistent with a depth-stratified model of subsurface viscosity, while DLEs in polewards of 45° have characteristics (i.e., high EM coupled with a positive correlation between EM and diameter) consistent with a low viscosity throughout an extensive depth, and they are likely strongly influenced by the desiccation of volatiles at lower obliquity (Jones and Osinski 2015). Our information is not sufficient to develop a new model. However, our observations support the hypothesis that the presence of volatiles within the regolith target materials is a factor in producing DLE craters.

MLE craters are typically larger and their ejecta are found at greater radial distances than SLE craters. The outermost layers of the MLE craters have high EM and Γ values, indicating that the ejecta material was very fluid at the time of emplacement. As in previous studies, it is suggested that the origin of multiple flows during the modification stage of crater formation is the result of heterogeneities in the target sequence of larger impact craters and/or instabilities in flow fronts (Wohletz and Sheridan 1983; Barlow and Bradley 1990; Osinski 2006; Weiss and Head 2014). One model for MLE craters is that they excavate into liquid water reservoirs (Barlow and Bradley 1990). Geomorphic investigations of fresh MLE craters indicate that their inner portions with their subtle rampart probably flowed similarly to their landslide counterparts as a basal glide (Barnouin-Jha et al. 2005). The lack of MLE craters on planetary bodies with little or no atmosphere, such as Ganymede (Neal and Barlow 2004), suggest that ejecta interaction with the atmosphere (Schultz 1992; Osinski 2006) may contribute to the formation of some MLE craters. On the other hand, the lack of MLE craters on Ganymede may also indicate that Ganymede does not have the same target variations with depth as Mars.

According to Barlow (2005), both subsurface volatiles and the thin Martian atmosphere may contribute to the morphologic, morphometric, and thermophysical properties of Martian layered ejecta craters. Compared with the previous study of Martian northern hemisphere craters (Barlow 2006), our global analysis of the layered ejecta craters on the entire Mars has resulted in both confirmation of Barlow's previous observations and some new findings. This study indicates that EM values increase at higher latitudes in both the northern and the southern hemisphere, which could be consistent with the expected distributions of subsurface water or ice. SLE, DLE, and MLE craters in the mid–high latitudes of Mars all have larger EM values and smaller onset diameters than those in the equatorial region, the observed latitudinal variations in the EM values and onset diameter in the study probably reflect the increased poleward stability of Martian subsurface volatiles. Studies of the distribution of lobateness of layered ejecta and contiguous ejecta ramparts on Mars indicate that the observed variations can be correlated with changes in diameter and latitude (Kargel 1989). Our study shows that Γ values vary little with latitude but increase with increasing crater diameter. This lobateness-latitude relationship is in agreement with the finding of Barlow (1994), who computed the sinuosity of Martian rampart ejecta deposits and suggested that Martian lobate ejecta morphologies from impact into subsurface volatiles, although she could not rule out differences in ejecta lobateness as resulting from atmospheric interactions with the ejecta during the impact process. Barnouin-Jha and Schultz (1998) predicted that increasing lobateness

with crater diameter is a natural consequence of ejecta emplacement in an atmosphere. Wind tunnel experiments and numerical modeling suggested that larger impacts can develop more complicated vortices within the atmosphere, producing the numerous partial layers observed with MLE craters (Barnouin-Jha et al. 1999a, 1999b).

In summary, our survey of the distribution and characteristics of layered ejecta craters reveals that strong correlations exist between EM and latitude, and there is a latitudinal dependence of onset diameter. Our study of Martian layered ejecta craters provides more detailed information and insights of connection between the layered ejecta morphologies and the subsurface volatiles. At present, our information is not sufficiently developed to provide the exact content of subsurface volatiles. Study of subsurface volatile properties could be carried out using more detailed geomorphic investigations, particularly into the thicknesses and volumes of rampart blankets and their global distribution. Such issues will be investigated in future research. The Mars atmosphere and volatile evolution mission is expected to bring about further improvements in our knowledge of volatiles and the atmosphere on Mars.

CONCLUSIONS

This article presents a comprehensive analysis of the global distribution and morphological features of Martian layered ejecta craters. After manually locating all visible layered ejecta craters with a diameter greater than 1.5 km across the entire planet, we extracted the morphological parameters for all SLE, DLE, and MLE craters, respectively. On the basis of crater statistical studies, some interesting relationships between the parameters were determined. From this analysis, we can summarize the following observations regarding the distributions of layered ejecta craters on Mars.

- The broad distribution of SLE and MLE craters suggests that the formation of these craters is controlled by factors that occur globally. However, the distribution of DLE craters shows longitudinal dependence.
- There is latitudinal dependence for the EM values and onset diameters of layered ejecta craters. SLE, DLE, and MLE craters in the mid–high latitudes of Mars all have larger EM values and smaller onset diameters than those in the equatorial region, indicating a poleward concentration of subsurface volatiles.
- Our geomorphic analyses show that Γ values vary little with latitude but increase with increasing crater diameter, indicating that the rheological properties of SLE, DLE, and MLE ejecta are different.

The results of this study of Martian layered ejecta craters provide more detailed information and insights of connection between the layered ejecta morphologies and the subsurface volatiles.

Acknowledgments—The authors acknowledge the THEMIS and MOLA science teams and the Mars Crater Consortium for making the relevant data available. This research is funded by the National Natural Science Foundation of China (41472303).

Editorial Handling—Dr. Gordon Osinski

REFERENCES

Arvidson R. E., Coradini M., Carusi A., Coradini A., Fulchignoni M., Federico C., Funiciello R., and Salomone M. 1976. Latitudinal variation of wind erosion of crater ejecta deposits on Mars. *Icarus* 27:503–516.

Baloga S. M., Fagents S. A., and Mouginis-Mark P. J. 2005. Emplacement of Martian rampart deposits. *Journal of Geophysical Research* 110:E10001. doi:10.1029/2004JE002338.

Barlow N. G. 1988. Crater size-frequency distributions and a revised Martian relative chronology. *Icarus* 75:285–305. doi:10.1016/0019-1035(88)90006-1.

Barlow N. G. 1994. Sinuosity of Martian rampart crater deposits. *Journal of Geophysical Research* 99:10,927–10,935.

Barlow N. G. 2004. Martian subsurface volatiles concentrations as a function of time: Clues from layered ejecta craters. *Geophysical Research Letters* 31:L05703. doi:10.1029/2003GRL19025.

Barlow N. G. 2005. A review of Martian rampart crater ejecta structures and their implications for target properties. In *Large Meteorite Impacts III*, edited by Kenkmann T., Hörz F., and Deutsch A. GSA Special Paper 384. Boulder, Colorado: Geological Society of America. pp. 433–442.

Barlow N. G. 2006. Impact craters in the northern hemisphere of Mars: Layered ejecta and central pit characteristics. *Meteoritics & Planetary Science* 41:1425–1436.

Barlow N. G. and Bradley T. L. 1990. Martian impact craters: Correlations of ejecta and interior morphologies with diameter, latitude, and terrain. *Icarus* 87:156–179.

Barlow N. G. and Perez C. B. 2003. Martian impact crater ejecta morphologies as indicators of the distribution of subsurface volatiles. *Journal of Geophysical Research* 108(E8):5085. doi:10.1029/2002JE002036.

Barlow N. G., Boyce J. M., Costard F. M., Craddock R. A., Garvin J. B., Sakimoto S. E. H., Kuzmin R. O., Roddy D. J., and Soderblom L. A. 2000. Standardization the nomenclature of Martian impact crater ejecta morphology. *Journal of Geophysical Research* 105:26,733–26,738.

Barlow N. G., Koroshetz J., and Dohm J. M. 2001. Variations in the onset diameter for Martian layered ejecta morphologies and their implications for subsurface volatile reservoirs. *Geophysical Research Letters* 28:3095–3098.

Barlow N. G., Boyce J. M., and Cornwall C. 2014. Martian low-aspect-ratio layered ejecta (LARLE) craters: Distribution,

characteristics, and relationship to pedestal craters. *Icarus* 239:186–200.

Barnouin-Jha O. S. and Schultz P. H. 1998. Lobateness of impact ejecta deposits from atmospheric interactions. *Journal of Geophysical Research* 103:25,739–25,756.

Barnouin-Jha O. S., Schultz P. H., and Lever J. H. 1999a. Investigating the interactions between an atmosphere and an ejecta curtain: 1. Wind tunnel tests. *Journal of Geophysical Research: Planets* 104(E11):27,105–27,115.

Barnouin-Jha O. S., Schultz P. H., and Lever J. H. 1999b. Investigating the interactions between an atmosphere and an ejecta curtain: 2. Numerical experiments. *Journal of Geophysical Research: Planets* 104(E11):27,117–27,131.

Barnouin-Jha O. S., Baloga S., and Glaze L. 2005. Comparing landslides to fluidized crater ejecta on Mars. *Journal of Geophysical Research* 110:E04010. doi:10.1029/2003JE002214.

Boyce J. M. 1979. A method for measuring heat flow in the Martian crust using impact crater morphology. *Reports of Planetary Geology Program* 1:114–118.

Boyce J. M. and Mouginis-Mark P. J. 2006. Martian craters viewed by the THEMIS instrument: Double-layered craters. *Journal of Geophysical Research* 111:E10005. doi:10.1029/2005JE2638.

Boyce J. M. and Witbeck N. E. 1980. Distribution of thermal gradient values in the equatorial region of Mars based on impact crater morphology. *Reports of Planetary Geology Program NASA TM-82385*, pp. 140–143.

Boyce J. M., Mouginis-Mark P., and Garbeil H. 2005. Ancient oceans in the northern lowlands of Mars: Evidence from impact crater depth/diameter relationships. *Journal of Geophysical Research: Planets* 110:E03008. doi:10.1029/2004JE002328.

Boyce J. M., Barlow N. G., Mouginis-Mark P. J., and Stewart S. 2010. Rampart craters on Ganymede: Their implications for fluidized ejecta emplacement. *Meteoritics & Planetary Science* 45:638–661.

Carr M. H., Crumpler L. S., Cutts J. A., Greeley R., Guest J. E., and Masursky H. 1977. Martian impact craters and emplacement of ejecta by surface flow. *Journal of Geophysical Research* 82:4055–4065.

Clifford S. M. and Hillel D. 1983. The stability of ground ice in the equatorial region of Mars. *Journal of Geophysical Research: Solid Earth* 88(B3):2456–2474.

Clifford S. M., Lasue J., Heggy E., Boisson J., McGovern P., and Max M. D. 2010. Depth of the Martian cryosphere: Revised estimates and implications for the existence and detection of subpermafrost groundwater. *Journal of Geophysical Research: Planets* 115(E7):E07001.

Costard F. M. 1989. The spatial distribution of volatiles in the Martian hydrolithosphere. *Earth, Moon, and Planets* 45:265–290.

Costard F. and Kargel J. 1995. Outwash plains and thermokarst on Mars. *Icarus* 114:93–112.

Fanale F. P., Salvail J. R., Zent A. P., and Postawko S. E. 1986. Global distribution and migration of subsurface ice on mars. *Icarus* 67:1–18.

Gault D. E. and Greeley R. 1978. Exploratory experiments of impact craters formed in viscous-liquid targets: Analogs for Martian rampart craters? *Icarus* 34:486–495.

Harrison T. N., Tornabene L. L., and Osinski G. R. 2013. Emplacement chronology of double layer cater ejecta on Mars (abstract #1702). 44th Lunar and Planetary Science. CD-ROM.

Jones E. and Osinski G. R. 2015. Using Martian single and double layered ejecta craters to probe subsurface stratigraphy. *Icarus* 247:260–278.

Kadish S. J., Barlow N. G., and Head J. W. 2009. Latitude dependence of Martian pedestal craters: Evidence for a sublimation-driven formation mechanism. *Journal of Geophysical Research-Planets* 114(E10):E10001.

Kargel J. S. 1989. First and second order equatorial symmetry of Martian rampart crater ejecta morphologies (abstract). 4th International Conference on Mars. Tucson, Arizona: The University of Arizona Press. pp. 132–133.

Komatsu G., Ori G. G., DiLorenzo S., Rossi A. P., and Neukum G. 2007. Combinations of processes responsible for Martian impact crater "layered structures" emplacement. *Journal of Geophysical Research* 112:E06005. doi:10.1029/2006JE002787.

Kuzmin R. O. 1980. Determination of frozen soil depth on Mars from the morphology of fresh craters. *Doklady Akademiia Nauk SSSR* 252:1445–1448.

Kuzmin R. O., Bobina N., Zabalueva E., and Shashkina V. 1988. Structural inhomogeneities of the Martian cryosphere. *Solar System Research* 22:121–133.

McCauley J. F. 1973. Mariner 9 evidence for wind erosion in the equatorial and mid-latitude regions of Mars. *Journal of Geophysical Research* 78:4123–4137.

Mellon M. T., Jakosky B. M., and Postawko S. E. 1997. The persistence of equatorial ground ice on Mars. *Journal of Geophysical Research: Planets* 102(E8):19,357–19,369.

Mouginis-Mark P. J. 1979. Martian fluidized ejecta morphology: Variations with crater size, latitude, and target materials. *Journal of Geophysical Research* 84:8011–8022.

Mouginis-Mark P. J. 1981. Ejecta emplacement and the modes of formation of Martian fluidized ejecta craters. *Icarus* 45:60–76.

Mouginis-Mark P. J. and Baloga S. M. 2006. Morphology and geometry of the distal ramparts of Martian impact craters. *Meteoritics & Planetary Science* 41:1469–1482.

Neal J. E. and Barlow N. G. 2004. Layered ejecta craters on Ganymede: Comparisons with Martian analogs (abstract #1337). 37th Lunar and Planetary Science. CD-ROM.

Osinski G. R. 2006. Effects of volatiles and target lithology on the generation and emplacement of crater-fill and ejecta deposits on Mars. *Meteoritics & Planetary Science* 41:1571–1586.

Osinski G. R., Tornabene L. L., and Grieve R. A. F. 2011. Impact ejecta emplacement on terrestrial planets. *Earth and Planetary Science Letters* 310:167–181.

Reiss D., Hauber E., Michael G., and Jaumann R. 2005. Small rampart craters in an equatorial region on Mars: Implications for near-surface water or ice. *Geophysical Research Letters* 32:L10202.

Robbins S. J. and Hynek B. M. 2012a. A new global database of Mars impact craters ≥1 km: 1. Database creation, properties, and parameters. *Journal of Geophysical Research* 117:E05004. doi:10.1029/2011JE003966.

Robbins S. J. and Hynek B. M. 2012b. A new global database of Mars impact craters ≥1 km: 2. Global crater properties and regional variations of the simple-to-complex transition diameter. *Journal of Geophysical Research* 117:E06001. doi:10.1029/2011JE003967.

Schorghofer N. and Aharonson O. 2005. Stability and exchange of subsurface ice on Mars. *Journal of Geophysical Research: Planets* 110(E5):E05003.

Schultz P. H. 1992. Atmospheric effects on ejecta emplacement. *Journal of Geophysical Research* 97:11,623–11,662.

Schultz P. and Gault D. 1979. Atmospheric effects on Martian ejecta emplacement. *Journal of Geophysical Research* 84:7669–7687.

Senft L. E. and Stewart S. T. 2008. Impact crater formation in icy layered terrains on Mars. *Meteoritics & Planetary Science* 43:1993–2013.

Shoemaker E. M. 1962. Interpretation of lunar craters. *Physics and astronomy of the Moon*, edited by Kopal Z. New York: Academic Press. pp. 283–359.

Stewart S. T. and Ahrens T. J. 2003. Shock Hugoniot of H_2O ice. *Geophysical Research Letters* 30:1332. doi:10.1029/2002GL016789.

Stewart S. T., O'Keefe J., and Ahrens T. 2001. The relation between rampart crater morphologies and the amount of subsurface ice (abstract #2092). 32nd Lunar and Planetary Science Conference. CD-ROM.

Wada K. and Barnouin-Jha O. S. 2006. The formation of fluidized ejecta on Mars by granular flow. *Meteoritics & Planetary Science* 41:1551–1569.

Weiss D. K. and Head J. W. 2013. Formation of double-layered ejecta craters on Mars: A glacial substrate model. *Geophysical Research Letters* 40:3819–3824.

Weiss D. K. and Head J. W. 2014. Ejecta mobility of layered ejecta craters on Mars: Assessing the influence of snow and ice deposits. *Icarus* 233:131–146.

Wohletz K. H. and Sheridan M. F. 1983. Martian rampart crater ejecta: Experiments and analysis of melt-water interactions. *Icarus* 56:15–37.

Wulf G. and Kenkmann T. 2014. A new phenomenological ejecta excavation and emplacement model for DLE craters (abstract #1792). 45th Lunar and Planetary Science Conference. CD-ROM.